Monte Carlo Simulations in Support of the Shuttle Upper Atmospheric Mass Spectrometer Experiment

James N. Moss*
NASA Langley Research Center, Hampton, Virginia
and
Graeme A. Bird†
University of Sydney, Sydney, Australia

This paper presents the results of calculations obtained with a direct simulation Monte Carlo (DSMC) method that describes both the external flow about the nose region of the Shuttle orbiter and the initial path between the shock-processed gases and a mass spectrometer mounted inside the orbiter. A dedicated, three-dimensional version of the DSMC was developed during the present study for the internal flow simulation along with the procedure for interfacing external and internal flows. The calculations spanning the hypersonic transitional flow regime (140–95 km altitude range) were for a multicomponent gas mixture consisting of five chemical species while simulating the effects of translational, rotational, vibrational, and chemical nonequilibrium. Results show that, within the entry region of the inlet tube where the gas has equilibrated with the sidewall tube temperature, the pressure is substantially less than pressure at the external surface. This pressure correction for the entry region is significant for all conditions investigated and increases with altitude. Results of parametric studies show the sensitivity of the equilibrated inlet sidewall pressure to mass flow rates, gas-surface reflection model, and tube sidewall temperature variations.

Nomenclature

A_b = base area
C_D = drag coefficient, F_x/qA_b
C_f = friction coefficient, τ/q
C_H = heat-transfer coefficient $2\dot{q}/\rho_\infty U_\infty^3$
C_i = mass fraction of species i, ρ_i/ρ
C_p = pressure coefficient, p/q
d = nominal molecular diameter
D = tube inside diameter
F = force
L = tube length
M = molecular weight of mixture
$\dot{m}$ = mass flow rate
p = pressure
R_N = nose radius
q = dynamic pressure, $\rho_\infty U_\infty^2/2$
$\dot{q}$ = heat flux
R = universal gas constant, R = 8.3143 J/mol K
S_∞ = speed ratio, $U_\infty/\sqrt{M/2RT}$
T = thermodynamic temperature
T_{ov} = overall kinetic temperature
u = velocity component tangent to body surface
U_∞ = freestream velocity
v = velocity component normal to body surface
X_i = mole fraction of species i
x = coordinate measured along the body centerline
x/L = nondimensionalized Space Shuttle orbiter axial length
α = angle of incidence
η = coordinate normal to body surface
θ = hyperboloid asymptotic half-angle
λ_∞ = freestream mean-free path
λ_1 = mean-free path adjacent to body surface
ρ = density
σ = total collision cross section
τ = shear stress
ϕ = azimuth angle

Subscripts

E = condition where gas temperature is equilibrated with sidewall temperature
i = ith species
s = surface value
∞ = freestream value

Introduction

THE Space Shuttle orbiter provides a means of making repeated measurements throughout the flow spectrum—encompassing free-molecule through continuum flow regimes. Two NASA orbiter experiments will utilize this capability to obtain information so that aerodynamic force coefficients can be extracted directly from measurements made in the free molecule and most of the transitional regimes. Force measurements are being obtained with the High Resolution Accelerometer Package (HiRAP) experiment[1] that has been flown on several Shuttle missions. The determination of the force coefficients requires an independent knowledge of the dynamic pressure. Knowledge concerning both the freestream density and dynamic pressure is to be obtained by a companion experiment called the Shuttle Upper Atmospheric Mass Spectrometer[2] (SUMS) that is scheduled for flight on orbiter 102 (Columbia) once the Shuttle flight program is resumed.

The objective of the SUMS experiment is to relate the measurements of the mass spectrometer to freestream density and dynamic pressure. The data reduction procedure for the

Presented as Paper 85-0968 at the AIAA 20th Thermophysics Conference, Williamsburg, VA, June 19–21, 1985; received April 1, 1986; revision received Dec. 8, 1986. Copyright ©1987 American Institute of Aeronautics and Astronautics, Inc. No copyright is asserted in the United States under Title 17, U.S. Code. The U.S. Government has a royalty-free license to exercise all rights under the copyright claimed herein for Governmental purposes. All other rights are reserved by the copyright owner.

*Research Engineer, Aerothermodynamics Branch, Space Systems Division. Associate Fellow AIAA.
†Professor, Department of Aeronautical Engineering. Associate Fellow AIAA.

SUMS experiment is one in which response of the mass spectrometer will be related to inlet pressure, and the inlet pressure, in turn, will be related to the freestream dynamic pressure q by means of a numerically derived relationship that relates the inlet pressure coefficient with the inlet pressure $[(Cp)_E = p_E/q_\infty \text{ vs } p_E]$. With the freestream dynamic pressure known, the freestream density is extracted directly, since the velocity of the orbiter is known with considerable accuracy. The benefits of improved knowledge of the aerodynamic force coefficients and knowledge of the density in the transitional flow regime are readily evident in predicting and interpreting performance of vehicles in hypersonic rarefied flows. Furthermore, improved knowledge of the freestream density in the 160–90 km range will significantly improve the basis for comparing calculations with flight data. This is particularly true since significant variations (± 40%) in freestream density with respect to atmospheric model values have been observed[1] for several orbiter reentries in this altitude range.

The SUMS objectives will be accomplished by sampling the shock-layer gases that enter an inlet tube connected to additional plumbing that provides the path to the mass spectrometer, which is remotely located with respect to the surface. The gases that enter the inlet tube will be in a nonequilibrium state throughout the altitude range for which the SUMS experiment will be operational (160–90 km). At some distance within the inlet tube, the gas will have undergone a sufficient number of collisions with the tube sidewall to have thermally equilibrated with the sidewall temperature. The numerical simulation discussed herein is concerned with calculating the pressure within the inlet tube for given freestream conditions, orbiter angle of incidence, and both surface and tube sidewall temperature distributions.

The importance of knowing the equilibrated tube pressure as a function of entry conditions is critical to the success of the SUMS experiment. This occurs because the overall characteristics (time lags, pressure drops, etc.) of the SUMS system have been determined in ground-based experiments using both static and dynamic tests for various gases where the entry conditions are always equilibrated with respect to the inlet tube temperature. For the flight case, the pressure where the gas is thermally equilibrated in the inlet corresponds to the imposed inlet pressure in the ground-based experiments; therefore, the equilibrated inlet pressure is the critical link between the SUMS response and the freestream conditions.

The link between the inlet pressure and freestream conditions is accomplished by numerical simulation studies using the DSMC method. Bienkowski carried on the numerical simulation work for several years, and the results of this activity are summarized in Refs. 3 and 4. He obtained the inlet pressure coefficient $(C_p)_E$ relationship with the inlet pressure p_E for nominal flight conditions, but had not initiated the sensitivity studies for parametric variations of important or poorly defined parameters prior to his recent death. Consequently, the present authors are conducting the numerical simulation studies in support of the SUMS experiment.

Several significant differences exist in the computer codes and the problem formulation as exercised in the present study and that reported in Refs. 3 and 4. The current calculations for both the external and internal flow utilize the DSMC method developed by Bird,[5-8] which accounts for a reacting five-component gas mixture while including rotational and vibrational excitation for the molecular species. Bienkowski used a single constituent with average O_2–N_2 cross sections while accounting only for rotational excitation. Another significant difference is the manner in which the external flow is coupled with flow in the inlet tube. Instead of modeling the input flux as a sum of two Maxwellian distributions fitted to the "perturbed" and "unperturbed" incident fluxes from the external flow, the present procedure stores (on a file) information from the external flow solution concerning the particles (atoms and molecules) that strike the surface element, which is at the same orientation as the inlet. Then, this particle file, containing information on 2×10^3 particles, is sampled on a random basis to obtain the mass flux of the particles that enter the tube from the external flowfield. The manner in which this boundary condition is simulated is important because translational nonequilibrium effects persist over the entire altitude range of the SUMS experiment.

Results presented in Ref. 9 included structure of the flowfield within the shock layer at the SUMS inlet location, whereas the present paper focuses only on the inlet tube. The sensitivity of the tube sidewall pressure is demonstrated for variations in tube mass flow rate, sidewall temperature distributions, and sidewall reflection model. Comparison of present results with those of Bienkowski[3] shows the same qualitative behavior, but the tube pressure results are appreciably different at the low altitudes.

The SUMS Experiment

A description of the elements of the SUMS experiment and its operational characteristics is given in Ref. 2. This section briefly describes some of the features of the SUMS system and its operation. As depicted in Fig. 1, the SUMS inlet tube is located aft of the nose cap along the windward side of the vehicle at an $\bar{x}/\bar{L}$ location of 0.025. Figure 2 is a simplified sche-

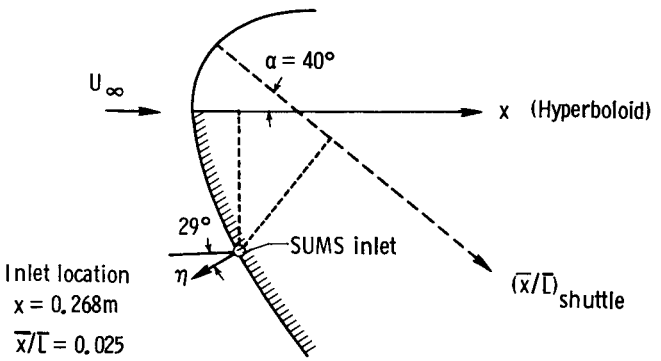

Fig. 1 Nose region geometry: Shuttle orbiter, hyperboloid, and SUMS inlet.

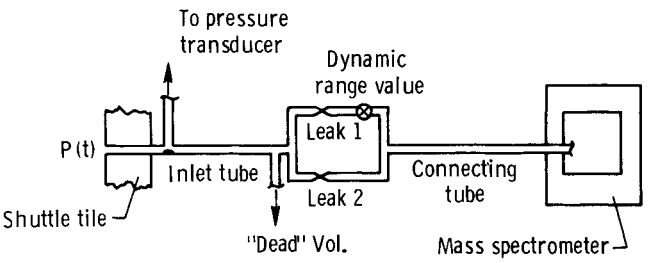

Fig. 2 Basic elements of SUMS system.

Table 1 Variable hard sphere (VHS) reference conditions

Parameters	External flow	Tube flow
Reference temperature, K	2880	288
Viscocity temperature exponent (S)	0.73	0.75
Reference diameter in meters for species		
O_2	3.062×10^{-10}	3.96×10^{-10}
N_2	3.083×10^{-10}	4.07×10^{-10}
O	2.297×10^{-10}	3.00×10^{-10}
N	2.398×10^{-10}	3.00×10^{-10}
NO	3.065×10^{-10}	4.00×10^{-10}

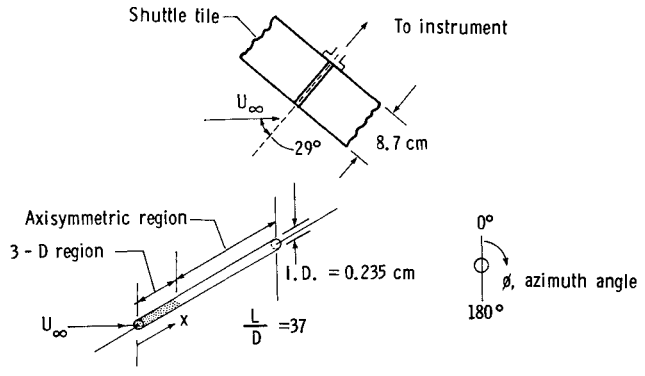

Fig. 3 Schematic representation of SUMS inlet tube.

matic of the elements of the experiment that shows the inlet system and mass spectrometer remotely located with respect to the inlet tube. The path length from the inlet to the mass spectrometer is rather long (approximately 1.24 m) and the temperature of most of the plumbing is relatively cold (approximately 300 K). Consequently, the atomic species that enter the inlet tube will have recombined before they reach the mass spectrometer. Normally, a mass spectrometer operates under high-vacuum conditions; yet, the SUMS experiment has been designed to operate at inlet pressures up to 80 Pa. This capability, which increases the altitude range for data extraction, is achieved by a specially designed inlet system to control the inlet gas flow and effectively create a "closed-source" mass spectrometer system.[2] The realization of this capability is through the use of two flow restrictors, or "leaks," in parallel.

The numerical simulation focuses on the external flowfield and the flow within the inlet tube. Also, only that portion of the inlet tube that is within the tile (Fig. 3) is considered. This portion of the tube is made of Vycor glass with an inside diameter of 0.235 cm and a length of 8.7 cm (L/D = 37). The orientation of the tube axis with respect to the freestream velocity vector is 29 deg. Flow in the initial portion of the inlet tube is three-dimensional, yet symmetric about the ϕ equal 0 to 180 deg diameter (Fig. 3).

Analysis

In the DSMC method, the intermolecular collisions are assessed on a probabilistic rather than a deterministic basis. A detailed description of the method is provided by Bird.[8] References 5 and 7 review the effects of molecular complexity on the results from previous simulations in which the molecular models for monatomic gases range from the hard sphere to those including long-range attractive forces. The effects appear to be fully explained through the variation of collision cross section with relative speed or temperature. Consequently, the "variable hard sphere" (VHS) model (Ref. 7) is now recommended for simulation of monatomic gases in an engineering context. The VHS model has a well-defined diameter and follows the classical hard sphere scattering law, but the diameter is an inverse power law function of the relative collision energy between the colliding molecules, i.e.,

$$\sigma \equiv \pi d^2 \propto \left(\frac{1}{2} M_r C_r^2\right)^{-\omega} \tag{1}$$

where M_r is reduced mass and C_r is collision relative speed. The power exponent of the inverse law, molecular force, is directly related to ω as is the temperature exponent of the coefficient of viscosity S by

$$S = \omega + \frac{1}{2} \tag{2}$$

Ultimately, the cross section can be expressed in terms of reference values and the collision speed as given by

$$\sigma = \sigma_{\text{ref}} \left\{ M_r C_r^2 \left[2(2-\omega) K T_{\text{ref}}\right] \right\}^{-\omega} \tag{3}$$

The parameters in the VHS model are chosen to match the viscosity coefficient in the real gas over the temperature range of interest. Table 1 lists the values used in the present calculations for d_{ref}, T_{ref}, and S. The values listed for the external flow were those that gave the best fit for the viscosity data recommended by Biolsi[10] for high temperature air species based on an exponential repulsive potential and the collision integrals recommended by Cubley and Mason.[11] The values listed for the tube flow are those that have been used in previous calculations, particularly for low energy flows.

For diatomic and polyatomic gases, the establishment of adequate models has proven to be difficult, and the difficulties associated with the physical models have led to development of phenomenological models of which the Larsen-Borgnakke[12] model is recommended for engineering studies. An outline of this model in a form that is compatible with a gas mixture of VHS molecules is given in Ref. 7.

The classical collision theory for chemical reaction rates is essentially a phenomenological approach based on steric factors or reactive cross sections and can be readily incorporated into direct-simulation methods. The expressions for the steric factors are developed in Ref. 8 for hard spheres and inverse power law models, whereas results for VHS models are given in Ref. 7.

The VHS model, along with the compatible Larsen-Borganakke model, and reactive cross sections are the molecular models used in the present Monte Carlo simulations.

Conditions for Calculations

Three sets of freestream conditions with altitudes at 140, 110, and 95 km are used in the present calculations. The conditions are summarized in Table 2 and are representative of those experienced by the Space Shuttle orbiter during reentry. The freestream density, temperature, and composition are those given by Jacchia[13] for an exospheric temperature of 1200 K. Note that the composition is adjusted to that for the three dominant freestream species (O_2, N_2, and O). The flow is characterized by speed ratios of 11.6–22.6 and freestream Knudsen numbers (based on nose radius) of 15.4–0.05.

External Flow Conditions

All of the external flow calculations were made for the hyperboloid described in Table 2. The "equivalent axisymmetric body" concept is used to model the windward centerline of the Shuttle at a given angle of incidence α with an appropriate axisymmetric body at zero angle of incidence as indicated in Fig. 1. The nominal angle of incidence for the orbiter is 40 deg as it traverses the transitional flow regime. The present authors have found the three-dimensional effects along the windward centerline to be negligible, affording significant reduction in the computational effort.[14] Bienkowski[3] used this model for much of his development work; his final results were for a three-dimensional model.

The surface temperature distributions are specified based on previous shuttle flight measurements with thermocouples mounted in the tile coating. For the 140 km case, the wall temperature distribution was assumed constant at 300 K. The surface temperatures at the SUMS inlet are given in Table 2. For the external flow calculations, the surface is assumed, for the present study, to be noncatalytic. Also, the gas-surface interactions are assumed to be diffuse with full thermal accommodation. No parametric variations are made for the external flow calculations.

A plane view of the computational domain is depicted in Fig. 4. This domain consists of one or more arbitrary regions

Table 2 Conditions for numerical simulation
a) Freestream conditions

Parameters	Case 1	Case 2	Case 3
Altitude, km	140	110	95
Density, kg/m^3	3.86×10^{-9}	9.67×10^{-8}	1.42×10^{-6}
Velocity, km/s	7.50	7.49	7.50
Temperature, K	625	247	189
Mole fractions			
X_{O_2}	0.062	0.123	0.197
X_{N_2}	0.652	0.770	0.787
X_O	0.286	0.106	0.016
Molecular weight, g/mol	24.82	27.23	28.61
Speed ratio	11.6	19.3	22.6
Knudsen number, λ_∞/R_N	15.35	0.673	0.048

b) Conditions adjacent to SUMS inlet[a]

Parameters	Case 1	Case 2	Case 3
Density, kg/m^3	1.12×10^{-7}	7.82×10^{-6}	1.15×10^{-4}
Molecular weight, g/mol	25.7	27.5	24.6
Mean-free path, m	0.76	1.1×10^{-2}	6.8×10^{-4}
Overall kinetic temperature, K	1744	1253	1423
Surface temperature, K	300	450	950
Surface pressure, Pa	0.16	4.33	58.5

[a]Equation for body is: $y^2 = x^2 \tan^2\theta + 2R_N x$ where θ = 50 deg and R_N = 1.143 m.

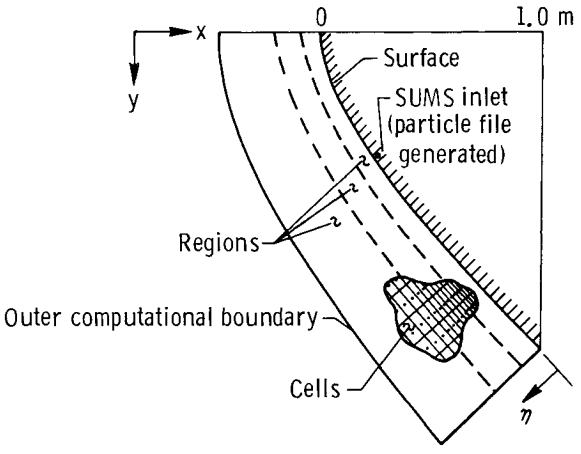

Fig. 4 External flow computational domain.

within which the time step, and the weighing factor that relate the number of computational molecules to the number of physical molecules, are a constant. The smallest unit of physical space is the cell that provides a convenient reference for the sampling of the macroscopic gas properties. The dimensions of the cells must be such that the change in flow properties across each cell is small. Time is advanced in discrete steps of magnitude such that the time step is small in comparison with the mean collision time.

The chemical kinetics model was the same as that used in Refs. 15 and 16 (the species O, O_2, N, N_2, and NO with 34 chemical reactions) where continuum computations with a viscous shock-layer analysis were shown to agree well with Shuttle flight measurements for altitudes lower than that considered in the present calculations.

Internal Flow Conditions

The high degree of nonequilibrium at the SUMS inlet tube precludes the use of surface conditions to describe the incident flux. Consequently, a particle file (molecules and atoms) is generated during the external flow calculation that is subsequently used to define the incident flow rate boundary condition for the tube by selecting particles at random from the particle file. The particle file serves as the link between the external and internal calculations.

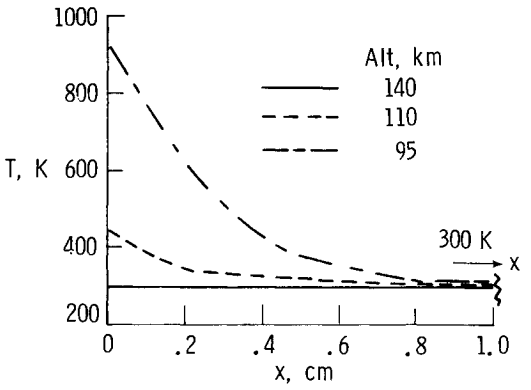

Fig. 5 Prescribed sidewall temperature distributions for inlet tube.

The initiation of the file generation occurs once the external flow calculation has reached steady flow. Then, as each particle strikes the surface element whose body normal is parallel to the tube axis, the following information for the particle is stored on the file: three velocity components, rotational energy, vibrational energy, and the kind of chemical species.

The axis of the inlet tube is 29 deg with respect to the freestream velocity vector; consequently, flow in the entry region of the tube will be three-dimensional. Initial calculations were made where the total length of the tube was treated as three-dimensional, which showed that the flow became axisymmetric a few tube diameters from the inlet. Consequently, the internal flow was described with a two-region code where the first region modeled the 3-D flow followed by the axisymmetric flow region. Most of the tube calculations used 9 azimuthal slices, 4 cells in the radial direction and 10 cells in the axial direction for the 3-D region, and 3 cells in the radial direction and 50 cells in the axial direction for the axisymmetric flow region.

The tube sidewall temperature distributions were specified according to the data shown in Fig. 5. Nominal conditions for the calculations were diffuse and noncatalytic sidewalls. Parametric variations from the nominal conditions included combinations of specular and diffuse reflection and sidewall temperatures different from those specified in Fig. 5.

The end boundary was always a diffuse surface with a temperature of 300 K. In addition, an absorbing boundary condition is exercised at the end of the tube to vary the exit flow rate. Zero absorption corresponds to a closed tube, whereas 100% absorption corresponds to a vacuum boundary. Since the ground-test simulations for the SUMS system indicated a nominal pressure drop of about 9% across the shuttle tile, this information was used to select an appropriate range of absorption values and to demonstrate the sensitivity of the tube pressure to the exit mass flow rate.

Results and Discussion

External Flow Results

The external flow results obtained show the same trends as results discussed in Ref. 14, and details of the present external calculations are included in Ref. 9. Briefly, the calculations show that thermodynamic nonequilibrium persists for the altitude range of the SUMS experiment and that gas-phase chemistry is significant only at the lower altitudes (below 105 km).

Internal Flow Results

Quasisteady conditions. An initial concern in the numerical simulation was whether the problem could be modeled as a

quasisteady problem. Since the nominal descent angle for the orbiter is 1.25 deg during the SUMS measurements, the altitude descent rate is approximately 160 m/s. Results of numerical tests show that steady flow is achieved in the entry region of the inlet tube within milliseconds (that corresponds to a negligible decrease in altitude) even though the overall response time for the SUMS system is on the order of seconds.[2] Furthermore, the time required to achieve steady flow decreases with decreasing altitude.

Entry region results. The flow is 3-D and undergoes significant changes within the first few diameters D along the inlet tube. An example of the azimuthal pressure distributions in the entry region, as a function of x/D, is shown for 110 km in Fig. 6. The corresponding results for the sidewall heat-transfer rates are presented in Fig. 7. Recall that symmetry exists along the diameter passing through $\phi = 0$ deg. Also, $\phi = 0$ deg receives the maximum shadowing effect, whereas $\phi = 180$ deg receives the maximum impact from the entry flow. Evidence of this is clearly demonstrated in Figs. 6 and 7. The calculated results show that within three tube diameters or less, the flow becomes axisymmetric. Furthermore, the distance required to achieve axisymmetric flow decreases with decreasing altitude.

Particle-surface collisions and particle-particle collisions are the two mechanisms by which the flow adjustments are made. At the highest altitude, the adjustments are primarily particle-surface interactions within the entry region, whereas at the two lower altitudes, both mechanisms are important.

Effect of mass flow rate and sidewall reflection. Results presented have been for a closed tube; however, the SUMS experiment will have a small but finite flow rate through the inlet tube. To duplicate the pressure drop within the inlet tube obtained in ground tests, the absorption boundary condition at the end of the tube was varied over a range of values. Figure 8 shows the results at 110 km for the modeled axisymmetric region flow where the absorption was varied from 0 to 1.0%. An absorption value of approximately 0.25% produces the desired pressure drop, and the corresponding flow rate is 7.36×10^{-12} kg/s. For the closed tube, the pressure in the modeled axisymmetric region was essentially constant. With increasing flow rate, pressure at the end of the tube drops; yet, as will be demonstrated in Fig. 10, the equilibrated sidewall pressure is insensitive to mass flow rates that are anticipated during the flight measurements.

Figure 9 shows the results of variations of the sidewall reflection model where different ratios of specular and diffuse reflection are assumed. The results are for a constant end absorption of 0.25%. As the specular component of reflection is increased, both the sidewall pressure and mass flow rate increase.

Of more concern is the sensitivity of the gas pressure p_E (equilibrated to the sidewall temperature) to variations in flow rate and reflection model. An example of these results is presented in Fig. 10 for an altitude of 110 km. The location of the equilibrated pressure ranged from $x/D = 2.5$-2.75 for the three cases considered. At the lower altitudes, the sidewall temperature gradients delay adjustment of the gas temperature to that of the sidewall value.

Equilibrated sidewall pressure was found to be a very weak function of flow rate (absorption boundary condition), particularly for flow rates corresponding to end absorption values of the order of 0.25%. However, the equilibrated pressure is sensitive to the assumption concerning the sidewall reflection model, i.e., pressure increases with increasing specular contribution as demonstrated in Fig. 10.

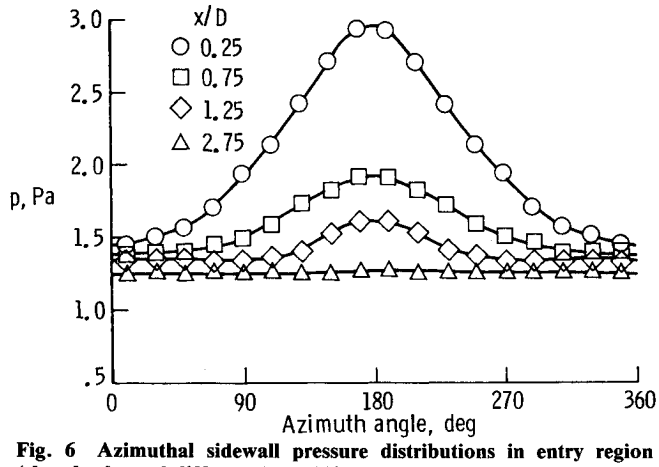

Fig. 6 Azimuthal sidewall pressure distributions in entry region (closed tube and diffuse, alt = 110 km, $P_s = 4.33$ Pa).

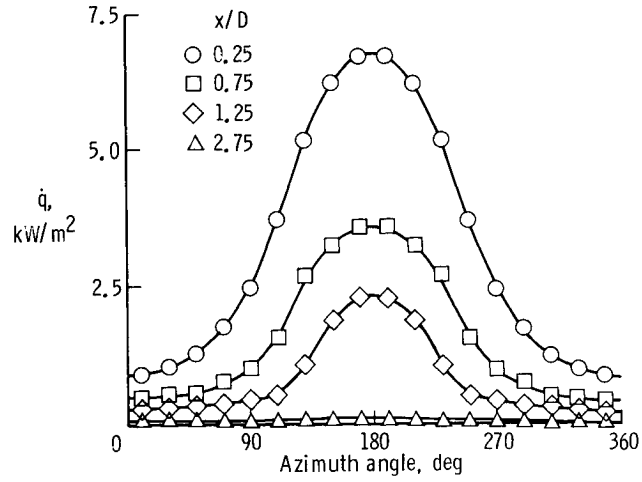

Fig. 7 Heat-transfer distributions in entry region (closed tube and diffuse, alt = 110 km, $q_s = 12.9$ kW/m^2).

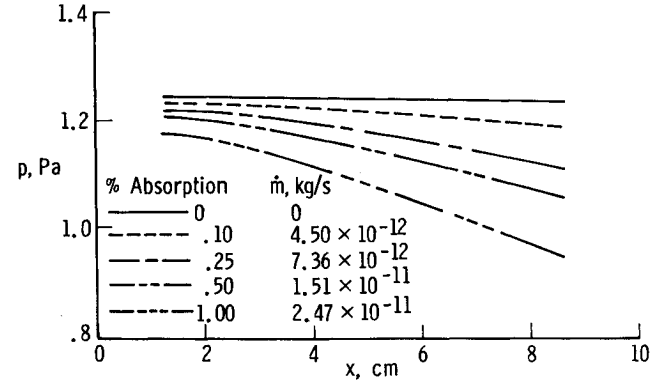

Fig. 8 Inlet tube pressure distributions as influenced by exit flow rate for the region modeled as being axisymmetric flow (alt = 110 km, diffuse sidewalls).

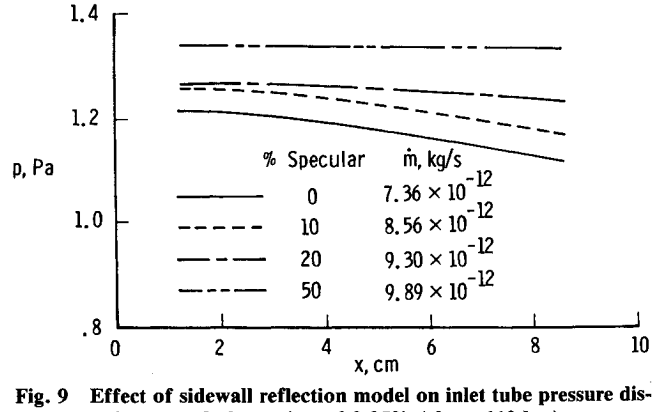

Fig. 9 Effect of sidewall reflection model on inlet tube pressure distributions for an end absorption of 0.25% (alt = 110 km).

Surface temperature effects. Sensitivity of the sidewall pressure to variations in surface temperature was examined for the 110 km case. The temperature variation consisted of using a constant sidewall temperature of 300 K rather than the distribution shown in Fig. 5. The overall effect is negligible in terms of tube mass flow rate (absorption = 0.25%) and pressure in the axisymmetric region ($x \geq 1.175$ cm). Therefore, the simulated results suggest that uncertainties in sidewall temperature variations would be a higher-order effect with negligible influence except possibly at the lowest altitudes (100–90 km).

Flow structure. Figure 11 presents results of the density and translational temperature profiles along a body normal extending into both external flow and the SUMS inlet tube. The density profile presented in Fig. 11a shows a continuous increase in density when moving from the external flow into the inlet tube.

The temperature profile across the inlet interface Fig. 11b experiences a much different behavior in that the temperature is essentially discontinuous at the interface. The discontinuities or jump effects develop whenever thermal nonequilibrium occurs.

Inlet pressure. Equilibrated tube pressure for the three altitudes considered is substantially less than the corresponding surface pressure. These results, in terms of pressure ratio p_E/p_s, are presented in Fig. 12. At 140 km, the calculated ratio is 0.16 and increases as the degree of rarefraction decreases. For continuum conditions in both the external and tube flows, the ratio would be unity.

The equilibrated tube pressure in a form appropriate for the SUMS data reduction[3] is presented in Fig. 13 together with those of Bienkowski.[3] With the results of ground-based tests providing the calibration of the response of the mass spectrometer to the equilibrated pressure in the inlet tube, the results of numerical simulations will provide the basis for linking this pressure to the freestream dynamic pressure. Such a relationship is demonstrated in Fig. 13 where the tube pressure coefficient is shown as a function of the tube pressure p_E. With the dynamic pressure extracted from this relation, the freestream density is directly available, since the vehicle velocity will be known with considerable accuracy. The freestream atmospheric properties, particularly density,[1] will probably differ significantly from those used in the current study; however, results correlated as in Fig. 13 will remove the dependence of atmospheric properties.

Comparison of Results

The numerical simulation studies by Bienkowski[3-4] are the only reported results for the present problem. The results of those calculations for the inlet tube pressure are low when compared with the present results (Fig. 13): 15% at 140 km and 30% at 95 km. However, surface pressures are in much

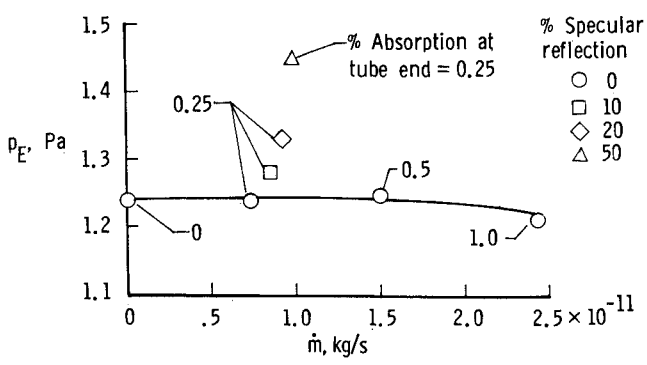

Fig. 10 Effect of mass flow rate (absorption) and sidewall reflection on equilibrated sidewall pressure (alt = 110 km, x/D = 2.75, P_s = 4.33 Pa).

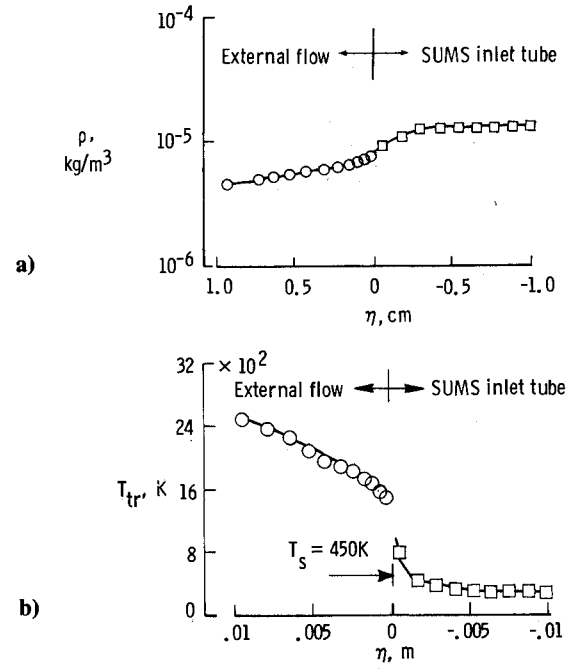

Fig. 11 Profiles of external and internal quantities along body normal (alt = 110 km, absorption = 0.25%); a) Density profile (ρ_∞ = 9.67×10^{-8} kg/m^3). b) Translational temperature profile.

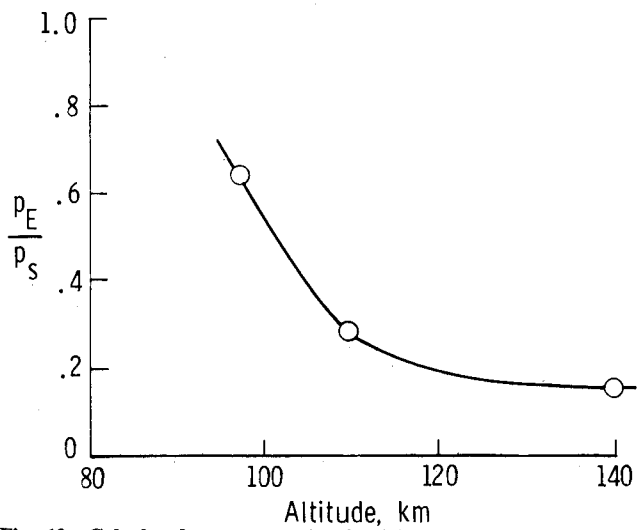

Fig. 12 Calculated pressure ratios for inlet tube with diffuse and noncatalytic sidewalls.

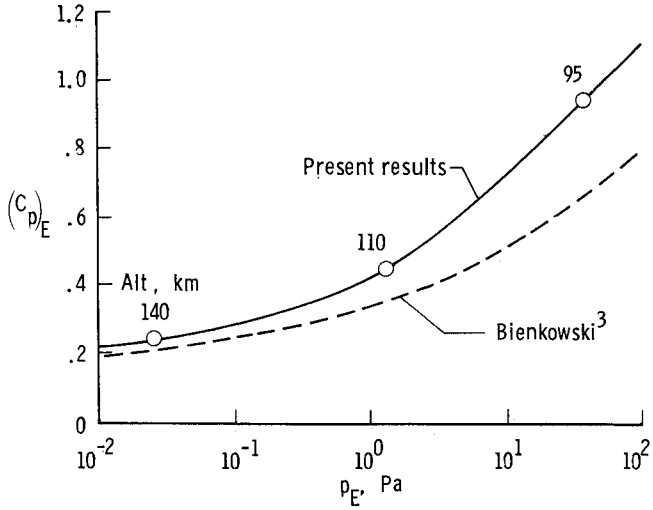

Fig. 13 Calculated data reduction curve for diffuse and noncatalytic sidewalls.

closer agreement; the results of Beinkowski are approximately 3% higher than the present results.

The disagreement is not unexpected since there are several differences between the two simulations in both the basic data and numerical parameters. Agreement in external surface pressures is not an adequate test, because surface pressure is the least sensitive of the surface parameters to variations in gas properties and numerical parameters in continuum or highly rarefied flows.

Significant differences between the two simulations were enumerated in the introduction; furthermore, for the tube problem, it appears that the previous study used the DSMC code for conditions at or below 95 km and used the free-molecule results of Hughes and deLeeuw[17] with the incident flux modeled in terms of the superposition of two drifting Maxwellian velocity distributions.

Present DSMC results for the stagnation-point heat-transfer coefficient at 95 km are approximately 50% of Ref. 4 results, strongly suggesting that Bienkowski's preliminary results for external flow were obtained with too coarse a grid. Parametric DSMC studies of Ref. 13 indicated computational cell size, collision cross sections, and their variations with relative collision speed (Eq. 3) to be important on calculated heating rates. Additionally, continuum no-slip viscous shock layer (VSL) results for the stagnation heat transfer are generally comparable to DSMC results at 95 km ($\lambda\infty/R_N = 0.055$) are in reasonable agreement with VSL calculations, in contrast to Ref. 4 results, which show an approximate factor of two greater for the DSMC solution. Final external DSMC calculations by Bienkowski were for a 3-D configuration, further suggesting the computational grid may have been too coarse, consistent with reasonable computing requirements.

During the development of the DSMC program to simulate internal tube flow, calculated results were compared with free-molecule impact results of Hughes and deLeeuw.[17] The uniform external flow was simulated as a multicomponent gas mixture under free-molecule flow conditions. The tube results compared favorably with the theory of Ref. 17.

The previous comparisons demonstrate that the calculated data are in agreement with theory for the free-molecule limit. For transitional flow, it is suggested that the present results are an improvement on those reported in Ref. 3 in the following respects: apparently better resolution of the external flow was obtained; more realistic expressions for viscosity were used to define the constants for the collision cross sections; and, more details were included in the simulation of the gas (multicomponent mixture, vibration, and chemical reactions).

Concluding Remarks

Through the use of two separate DSMC codes and a procedure for linking the two separate flow calculations, results have been obtained that provide a relation between the pressure inside the inlet tube as a function of the freestream dynamic pressure for the SUMS experiment. Results of these calculations show the following:

1) The inlet flow is equilibrated with the sidewall temperature within three tube diameters or less.

2) The inlet tube pressure is dependent on the nature of the gas-surface interaction, where the pressure and mass flow rate increase as the fraction of particles specularly reflected at the sidewall is increased. Also, the local external surface pressure under free-molecule conditions would increase directly as the fraction of specularly reflected particles increased.

3) The equilibrated tube pressure is not sensitive to the range of tube mass flow rates anticipated during the flight experiment.

4) Sidewall temperature variations appear to be higher-order perturbations on the equilibrated tube pressure.

5) The pressure in the inlet tube is substantially less than the surface pressure.

6) The time constant for the entry region of the inlet tube is on the order of milliseconds, permitting quasisteady modeling.

7) The data obtained are in qualitative agreement with previous calculations and provide quantitative improvements over the previous data.

Additional calculations for the 95 km case would be instructive where parametric variation in both sidewall temperature distributions and catalytic conditions are made. In addition, a calculation for this altitude should be made to estimate the dependence of the inlet tube flow to external surface recombination assumptions.

The nature of the gas-surface interaction is shown to affect the pressure throughout the inlet tube. Yet, to be more definitive, it is essential that experimental data be obtained that provide an understanding of the effect and how it can be modeled.

Acknowledgments

The authors wish to express their appreciation for the many contributions made by Robert Blanchard, Frank Brock, Roy Duckett, Edwin Hinson, and Ann Simmonds.

References

[1]Blanchard, R. C. and Buck, G. M., "Determination of Rarefied-Flow Aerodynamics of the Shuttle Orbiter from Flight Measurements on STS-6 and STS-7," AIAA Paper 85-0347, Jan. 1985.

[2]Blanchard, R. C., Duckett, R.J., and Hinson, E. W., "A Shuttle Upper Atmosphere Mass Spectrometer (SUMS) Experiment," AIAA Paper 82-1334, Aug. 1982.

[3]Bienkowski, G. K., "Inference of Free Stream Properties from Shuttle Upper Atmosphere Mass Spectrometer (SUMS) Experiment," *Rarefied Gas Dynamics,* Vol. 1, edited by Hakuro Oguchi, University of Tokyo Press, 1984, pp. 295-302.

[4]Bienkowski, G. K., "Investigation of the External Flow Analysis for Density Measurements at High Altitudes," NASA CR-172464, Nov. 1984.

[5]Bird, G. A., "Monte Carlo Simulation of Gas Flows," *Annual Review of Fluid Mechanics,* Vol. 10, edited by M. D. Van Dyke et al., Annual Reviews Inc., Palo Alto, CA, 1979, p. 11.

[6]Bird, G. A., "Simulation of Multi-Dimensional and Chemically Reacting Flows," *Rarefied Gas Dynamics,* Vol. 1, Commissariat A L'Energie Atomique, Paris, 1979.

[7]Bird, G. A., "Monte-Carlo Simulation in an Engineering Context," *AIAA Progress in Astronautics and Aeronautics: Rarefied Gas Dynamics,* Vol. 74, Pt. 1, edited by Sam S. Fisher, AIAA, New York, 1981, pp. 239-255.

[8]Bird, G. A. *Molecular Gas Dynamics,* Clarendon Press, Oxford, 1976.

[9]Moss, J. N. and Bird, G. A., "Monte Carlo Simulations in Support of the Shuttle Upper Atmospheric Mass Spectrometer Experiment," AIAA Paper 85-0968, June 1985.

[10]Biolsi, L., "Critique IV of the Transport Properties of Air," NASA NSG 1369, May 1982.

[11]Cubley, S. J. and Mason, E. A., "Atom-Molecule and Molecule-Molecule Potentials and Transport Collision Integrals for High-Temperature Air Species," *The Physics of Fluids,* Vol. 18, Sept. 1975.

[12]Borgnakke, C. and Larsen, P. S., "Statistical Collision Model for Monte Carlo Simulation of Polyatomic Gas Mixtures," *Journal of Computational Physics,* Vol. 18, 1975, pp. 405-420.

[13]Jacchia, L. G., "Thermospheric Temperature, Density, and Composition: New Models," *Research in Space Science,* Smithsonian Astrophysical Observatory Special Rept. No. 375, March 1977.

[14]Moss, J. N. and Bird, G. A., "Direct Simulation of Transitional Flow for Hypersonic Reentry Conditions," *Progress in Astronautics and Aeronautics: Thermal Design of Aeroassisted Orbital Transfer Vehicles,* Vol. 96, edited by H. F. Nelson, AIAA, New York, 1985, pp. 113-139.

[15]Shinn, J. L., Moss, J. N., and Simmonds, A. L., "Viscous Shock-Layer Heating Analysis for the Shuttle Windward Symmetry Plane with Surface Catalytic Recombination Rates," *Progress in Astronautics and Aeronautics: Entry Vehicle Heating and Thermal Protection Systems,* Vol. 85, edited by P. E. Bauer and H. E. Collicott, AIAA, New York, 1983, pp. 149-180.

[16]Zoby, E. V., Gupta, R. N., and Simmonds, A. L., "Temperature Reaction Rate Expressions for Oxygen Recombination," *Progress in Astronautics and Aeronautics: Thermal Design of Aeroassisted Orbital Transfer Vehicles,* Vol. 96, edited by H. F. Nelson, AIAA, New York, 1985, pp. 445-464.

[17]Hughes, P. C. and deLeeuw, J. H., "Theory for the Free Molecule Impact Probe at an Angle of Attack," *Rarefied Gas Dynamics,* Vol. 1, edited by J. H. deLeeuw, Academic Press, New York, 1965, pp. 653-676.